The Fracture Diagram: A New Design Tool for Stiffened Panels

M. M. Ghassem
Spring, Texas
and
T. P. Rich*
Bucknell University, Lewisburg, Pennsylvania

A detailed explanation is presented for the use of fracture diagrams in the design of stiffened panels. Based upon some recent work on the development of fracture diagrams for a large sheet containing a crack midway between two parallel, riveted stiffeners, this paper emphasizes a methodology for employing fracture diagrams to estimate maximum loads, critical flaw sizes, and fatigue life for stiffened panels. In addition, the fracture diagram approach enables failure predictions to be made ranging from linear elastic rapid crack propagation to net section failure at the ultimate strength level of the material. The fracture diagrams are dimensionless and can be used for any material where meaningful yield strength and fracture toughness properties are available. References are provided for background and theoretical development of the fracture diagram approach.

Introduction

OVER the past few decades the aircraft industry has devoted considerable effort to incorporate fracture control procedures into the design of their structures. One of the problems confronting aircraft designers is the modeling of the ductility effect into their fracture analysis. The fracture diagram approach is a new analytical method for predicting the failure of a structural component that can be modeled as a two-dimensional object containing a crack under mode I opening. The ductility of the component is taken into account through the use of a strip yield plastic zone employed at each crack tip. This plastic zone is similar to that first used by Dugdale[1] in his analysis of an unstiffened sheet under tension.

Rich et al.[2] recently have given a generalized derivation of the fracture diagram and discussed the insight possible into failure prediction from this approach. Briefly, their paper shows the energy required to begin the rapid, catastrophic propagation of a crack in a structural component as results from linear elastic fracture mechanics. It also develops the energy required to begin the rapid, ductile tearing of a cracked component as results from net section failure. The latter critical energy is derived in terms of a critical crack tip opening displacement (CTOD), whereas the former critical energy is given in terms of the plane strain fracture toughness K_{IC}. Through an assumption that failure of a real material involves energy input to break the actual mechanical bonds at a crack tip (both linear and nonlinear energy components), the critical energy as predicted by any model (linear elastic fracture mechanics or net section yielding) should be equivalent when referred to the crack tip. The mathematics as presented in Ref. 2 led to the following general relationship for two-dimensional, elastic-plastic, mode I failure.

$$\frac{K_I}{K_{IC}} = \frac{Q}{\sqrt{Q_\delta}} \frac{\sigma}{\sigma_Y} \left\{ \frac{8}{\pi^2} \ell n \sec\left(\frac{\pi\sigma}{2\sigma_Y} \right) \right\}^{-1/2} \tag{1}$$

where K_I/K_{IC} represents the ratio of the linear elastic stress intensity factor to the plane strain fracture toughness at failure; σ/σ_Y is the ratio of the applied stress remote and perpendicular to a crack to the material's yield strength (ultimate tensile strength or some other cohesive strength property). The Q and Q_δ terms are the geometry factors from the linear elastic stress intensity factor and the crack tip opening displacement solutions, respectively.

In effect,

$$Q = \frac{K_I \text{ (component in question)}}{K_I \text{ (infinite tensile sheet)}} \tag{2}$$

and

$$Q_\delta = \frac{\text{CTOD (component in question)}}{\text{CTOD (infinite tensile sheet)}} \tag{3}$$

where the infinite sheet solutions are given in the literature.[3-5] When plotted graphically Eq. (1) produces a locus of points termed the fracture diagram.

Other work[2,6,7] has provided the analytical results needed to determine Q and Q_δ for construction of fracture diagrams for one specific structural component of great interest to the aircraft industry, the stiffened panel under uniaxial tension. It is the intent of this paper to present a detailed explanation of the potential design usage of fracture diagrams for stiffened panels. For more detailed information on the underlying analysis, readers are referred to Ref. 2.

The remainder of this paper consists of four major parts. The first pertains to the graphical description of the fracture diagram for both stiffened and unstiffened panels. In addition, an illustration of a stiffened panel loaded with cracks of different sizes is presented on a fracture diagram. The second part discusses the applications of the fracture diagram with respect to design. Here an engineer can address either of two problems: the determination of maximum load and/or critical flaw size. The third part of the paper is devoted to a comparison of fracture diagram predictions with experimental results. The last section demonstrates the prediction of fatigue life of a stiffened panel using fracture diagrams.

Fracture Diagram: A Graphical Representation

The fracture diagram approach offers a means for predicting the fracture of many common structural components containing a crack. A fracture diagram can be utilized for post-mortem failure analysis and in preventive quality control, whereby design measures may be taken to avoid failure. In this paper fracture diagrams are given to predict the fracture of a stiffened[8] and an unstiffened panel

Received April 12, 1982; revision received Oct. 4, 1982.

*Associate Professor, Mechanical Engineering Department.

containing an existing crack. The fracture diagrams are theoretically based upon the crack opening displacement (COD) concept as given by Wells,[9] and the strip yield zone model for crack tip plasticity as proposed by Dugdale[1] leading to Eq. (1) as discussed earlier.

Figure 1 shows a typical fracture diagram for a stiffened panel. It is plotted as a ratio of stress intensity over fracture toughness (K_I/K_{IC}) vs a ratio of applied stress over yield strength (σ/σ_Y). The failure curve is defined for a specific ratio of existing half crack length over stiffener spacing a/b for a twin stiffened panel as defined by Fig. 2. The relative stiffness between the stiffener and the panel, μ, was set equal to

$$\mu=\frac{A_sE_S}{(A_sE_s+btE)}=0.5 \tag{4}$$

where A_s and E_S are the cross-sectional area and modulus of elasticity of the stiffener, respectively; t and E are thickness and modulus of elasticity of the panel, respectively; and b is stiffener spacing.

The fracture diagram is dependent upon some geometric and material parameters which were chosen to be representative of typical aircraft construction, and are given as follows: $p/b=0.16667$, $R/p=0.125$, and $p/p_0=1.0$.

Figure 2 shows the definition of the parameters, as well as the analytical modeling of the crack tip plasticity by a strip yield zone and material yield strength σ_Y. The dotted line in Fig. 1 represents a third degree curve fit for designing purposes. The points located beneath the failure curve are considered to be safe. The failure curve itself contains a locus of points representative of fracture response from purely elastic fracture ($K_I=K_{IC}$) to entirely ductile failure conditions ($\sigma=\sigma_Y$) for a center-cracked stiffened panel.

It should be noted that as a graphical representation of Eq. (1), the fracture diagram shown in Fig. 1 is the actual failure curve for any twin stiffened panel where $\mu=0.5$, $a/b=0.526$, and the other geometric parameters are as given before. It is not a schematic. In addition, it applies to any material where the yield strength and plane strain fracture toughness can be determined. Note that some flexibility exists in that the ultimate tensile strength can be used in place of σ_Y; if that is thought to be more representative of the net section failure strength for a given material or a plane stress fracture toughness, K_C can be used in place of K_{IC} for thin sheet material. As discussed in detail in Ref. 2, the ductile effect upon failure in the fracture diagram is not associated with plane stress but rather with the gross transition from brittle fracture to net section yielding and ultimate failure.

The fracture diagram for an unstiffened panel was given by the Central Electricity Generating Board[10](CEGB). This is shown in Fig. 3 as a dashed line, whereas the solid line curve represents the stiffened panel, again for $a/b=0.526$. In the case of the stiffened panels, the failure curve changes with the ratio of the crack size to the stiffener spacing. The curve for the unstiffened panel was obtained by using COD results for a crack in an infinite size panel. The unstiffened panel curve does not depend upon values of a/b; it is effectively the limiting case as a/b goes to zero for the stiffened panel curves. Note the ratio of K_I/K_{IC} for an unstiffened panel decreases from unity when the load ratio increases. As seen from Fig. 3, in the case of a stiffened panel, the value of K_I/K_{IC} may go above unity as the load ratio σ/σ_Y increases, and it reaches a peak value before both the stiffened and the unstiffened curves go to zero. The slope of the fracture diagrams is, indeed, steep as σ/σ_Y approaches unity. It was shown in Ref. 2 that both numerically and analytically, K_I/K_{IC} approaches zero.

Figure 4 shows plots of the actual fracture diagrams for different crack sizes. The lowest curve is for an unstiffened panel with $a/b\to 0$. The next curve is for a stiffened panel with $a/b=0.1$; the crack size is small and far from the stiffener. Its

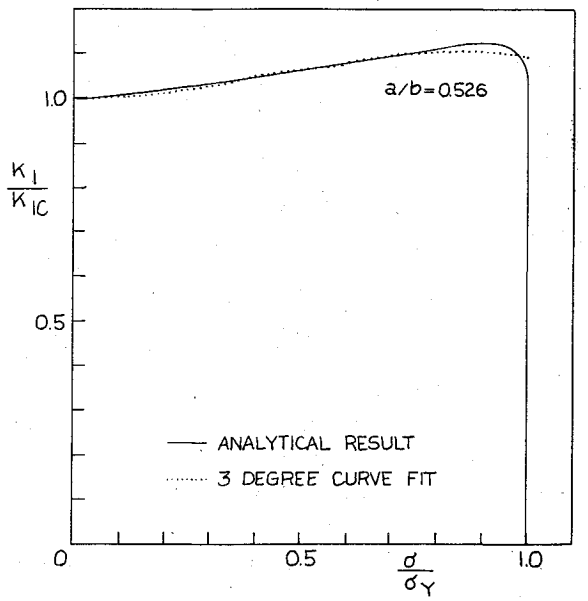

Fig. 1 Fracture diagram for a twin stiffened panel, $\mu=0.5$ and $a/b=0.526$.

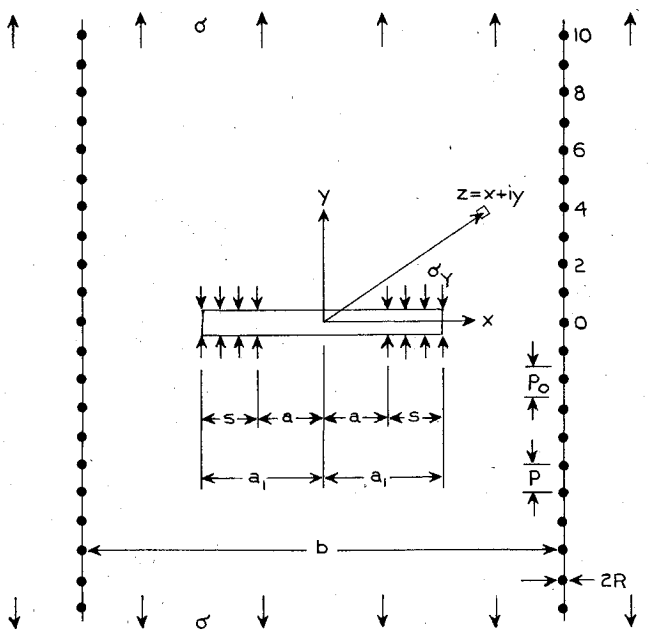

Fig. 2 Cracked, twin stiffened panel with strip yield zones.

effect is not as significant at the lower loads as for the higher load ratios. When the applied load increases, the effect of the stiffener becomes stronger and results in the separation of the stiffened curve from the unstiffened curve, until eventually, the curve reaches the limit where $\sigma=\sigma_Y$ and $K_I/K_{IC}=0$. The third curve is for $a/b=0.25$; with an increased crack size, the distance between the crack tip and the stiffener becomes less. The effect of the stiffener increases, and the curve does not go to lower values of K_I/K_{IC} until σ/σ_Y is almost unity. For $a/b=0.526$, the crack is slightly past the stiffener and the influence of the stiffener is greatest. According to Poe,[6] the stiffener's effect on stress intensity factor is maximum when the crack is just past the stiffener, as illustrated in Fig. 5. In the case of $a/b=0.667$, the crack tip has passed the stiffener, whose effect therefore diminishes. For $a/b=0.85$, the crack size has increased well past the stiffener; its effect decreases back toward the unstiffened case.

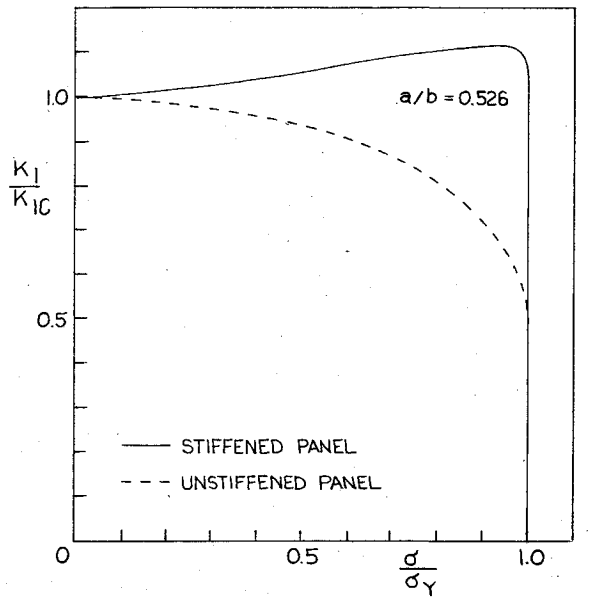

Fig. 3 Comparison of fracture diagrams, stiffened vs unstiffened panels.

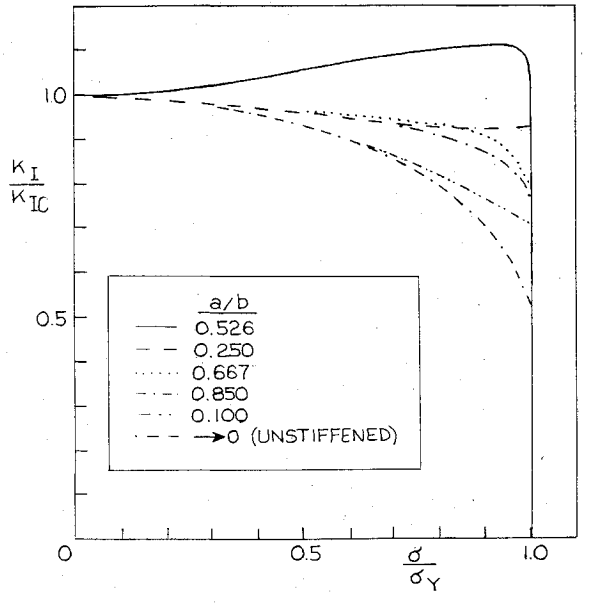

Fig. 4 Summary of fracture diagrams for stiffened panels, $\mu = 0.5$.

A fracture diagram represents three fracture mechanisms: 1) when the applied stress to yield strength is close to zero, the fracture mechanism is controlled by linear elastic fracture mechanics (LEFM) and the propagation of a dominant elastic crack; 2) when the applied stress to yield strength increases, the fracture mechanism is controlled by COD and a transition to ductile crack propagation; and 3) when the applied load to the yield strength ratio is close to one, the fracture mechanism is controlled by net section yielding.

Fracture Diagrams in Design

A fracture diagram gives a designer a new tool to predict the fracture of structures and may be used for both brittle and ductile failures. One objective in design of a structure is to optimize performance relative to costs. These include the cost of the materials, design, fabrication, operation, and maintenance. The engineering goal is to produce a structure that will perform the operating function efficiently, economically, and safely. One important prediction which engineers must make is based upon the loads and subsequent stresses that will cause functional failure of the structure. Many failures result from a flaw or crack, that initially had been introduced during fabrication, processing, and/or operations. Under cyclic loading, which often is below the yield strength, a crack grows larger and eventually causes failure.

The fracture diagram can be a very useful tool in design and quality control considerations by enabling an engineer to address either of two distinct design situations. In the first design case, it is assumed that a designer knows the component's shape and dimensions, and that he wants to calculate the maximum load for an assumed flaw size located in the

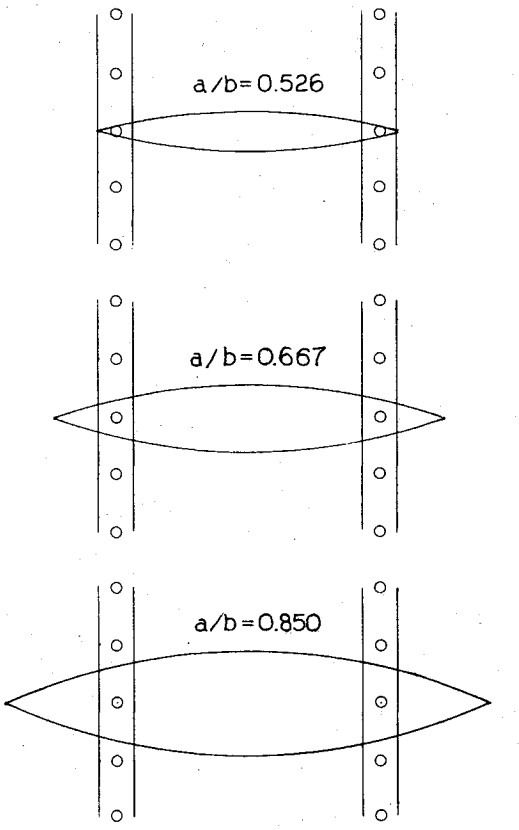

Fig. 5 Location of cracks with respect to stiffness.

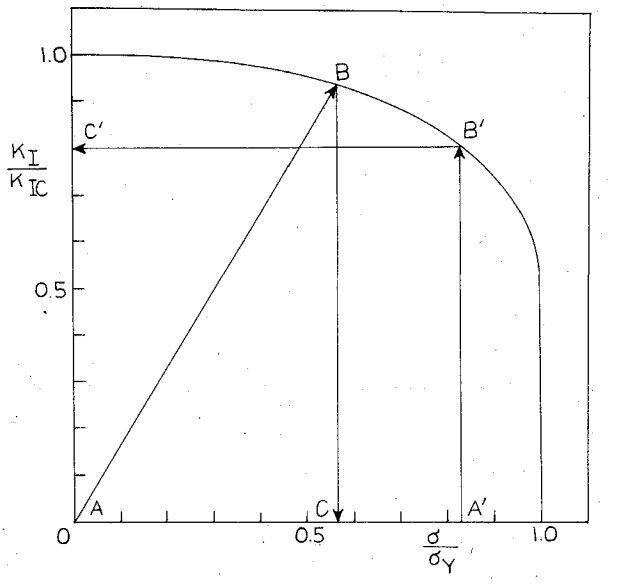

Fig. 6 Use of a fracture diagram in design (unstiffened panel).

component. In the second design case, it is assumed that the designer knows the maximum design load that will be acting on a component, and that he wants to determine the critical flaw size. In order to determine maximum load and the critical crack size, it is necessary to know the stress intensity factor for a given structural geometry and loading. The general form of the stress intensity factor is a function of geometry Q, nominal load σ, and crack size a. It can be written as

$$K_I = Q\sigma\sqrt{\pi a} \tag{5}$$

The ratio of stress intensity over fracture toughness is given as

$$K_I/K_{IC} = Q\sigma\sqrt{\pi a}/K_{IC} \tag{6}$$

For illustration purposes, the unstiffened panel fracture diagram is given alone in Fig. 6. For design case 1, at a given crack size the critical load is determined by constructing a slanted line from the origin, point A, whose slope is determined from Eq. (6) to be

$$(K_I/K_{IC})/(\sigma/\sigma_Y) = Q\sigma_Y\sqrt{\pi a}/K_{IC} \tag{7}$$

The point of intersection between the slanted loading path and the fracture diagram, point B, is located. A vertical line is drawn downward and the critical load ratio, σ_f/σ_Y, is obtained at point C. Given that the material yield strength is known, the critical load stress σ_f is obtained. Therefore, a designer could determine the maximum load to cause failure.

Alternately, one could calculate the critical crack size under service maximum load conditions for design case 2. To determine the critical crack size the designer first establishes the value of the operation load ratio, σ_f/σ_Y, shown as point A′ in Fig. 6. Next, he draws a vertical line from A′ to locate the intersection of the fracture diagram at B′. Finally, he draws a horizontal line to intersect the K_I/K_{IC} axis at point C′. By knowing the stress intensity function in terms of its crack size, load, and geometry, the critical crack size is found from the root of the equation

$$K_I = Q\sigma\sqrt{\pi a} = K_{IC}(K_I/K_{IC}) \tag{8}$$

It should be mentioned again that, in general, a fracture diagram is dependent upon the values of the geometric parameters of the component; when they change, the fracture diagram alters accordingly. The advantage of using a stiffened vs an unstiffened panel in a structure can be observed from the appropriate fracture diagram. Use of a stiffener in the structure allows the designer more safe space inside of the fracture envelope than for the unstiffened panel. For instance, for $a/b = 0.526$, Fig. 3 shows that there is extra safe space for a stiffened panel at points where failure would have occurred for the unstiffened panel.

As an aid to designers interested in applying the new fracture diagrams, Table 1 gives the coefficients of a third degree polynomial using a least square fit to each curve. The general representation for each diagram is

$$\frac{K_I}{K_{IC}} = A_0 + A_1\left(\frac{\sigma}{\sigma_Y}\right) + A_2\left(\frac{\sigma}{\sigma_Y}\right)^2 + A_3\left(\frac{\sigma}{\sigma_Y}\right)^3 \tag{9}$$

Comparison of Fracture Diagram Predictions with Experimental Results

The experimental results by Feddersen[11] on aluminum tension panels has been used to evaluate the fracture diagram. The panels tested were 914 mm (36 in.) wide and 2.54 mm (0.1 in.) thick. They were made of 7075-T6 alloy, $\sigma_Y = 517$ MNm^{-2} (75 ksi), and $K_{IC} = 77$ MNm$^{-3/2}$ (70 ksi $\sqrt{\text{in.}}$). The comparison is very informative, with the fracture diagram offering the potential for closer approximation of panel strength for small crack sizes than is possible from LEFM. For large cracks, both the LEFM and the fracture diagram gave good results compared to experimental values. Figure 7 shows a solid line that was determined for fracture of an unstiffened panel from the fracture diagram and the dashed line that was determined by LEFM. The dots represent the experimental values.

For smaller crack sizes, LEFM cannot predict the fracture stress since it goes to infinity, whereas the fracture diagram approaches σ_Y or the ultimate tensile strength if it is used as the limiting strength. The reason for this is that in LEFM, the stress intensity approach does not take into consideration failure from net section yielding as does the fracture diagram. Rather, LEFM always assumes failure from the brittle propagation of an elastic crack.

In Feddersen's experiment the crack sizes were given, and the fracture stresses were experimentally determined (design case 1). In order to determine the residual stress (fracture stress) from the fracture diagram, it is necessary to know the stress intensity, the fracture toughness, and yield strength. The ratios K_I/K_{IC} and σ/σ_Y can be defined as functions of the load stress σ. Since there is a linear relationship between K_I/K_{IC} and σ/σ_Y, as shown in Eq. (7), the load paths result in a straight line for each given crack size, as shown in Fig. 8. The points of intersection of the loading paths and fracture diagram were located; hence σ_f values were calculated.

In Fig. 7 when the crack size is large, the fracture stress is small. The ratio σ/σ_Y at failure also is small; the fracture occurs where LEFM gives good results, with the appropriate value for fracture toughness, as does the fracture diagram.

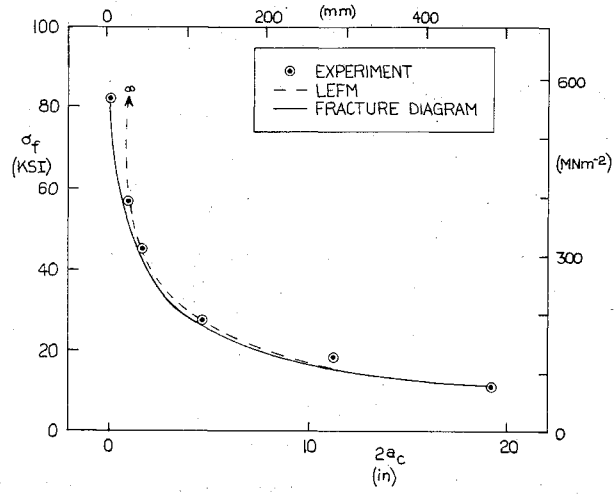

Fig. 7 Comparison of failure theories with experimental results for unstiffened aluminum alloy panels.

Table 1 Coefficients of third degree polynomial curve fit

a/b	0	0.1	0.25	0.526	0.667	0.85
A_0	1.0121	1.0009	0.9978	1.0106	1.0093	1.0052
A_1	−0.3284	0.0217	0.0815	−0.0782	−0.1327	−0.1307
A_2	0.9807	−0.2120	−0.4148	0.5924	0.3070	0.3273
A_3	−1.0940	−0.0896	0.2713	0.4320	−0.3376	−0.3876

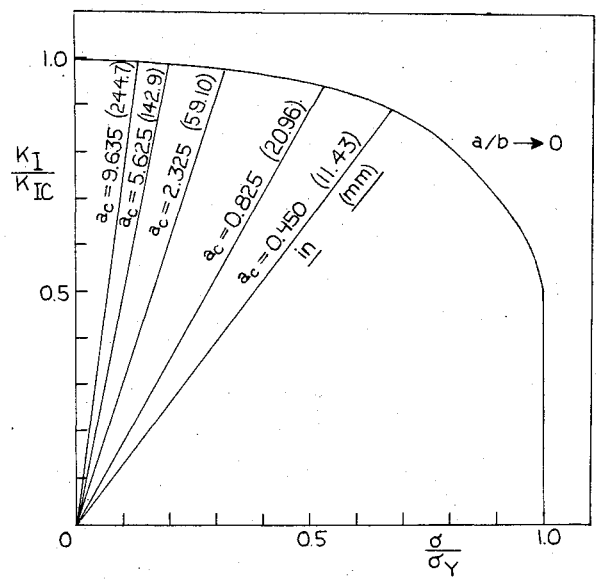

Fig. 8 Application of the fracture diagram to Feddersen experimental data.

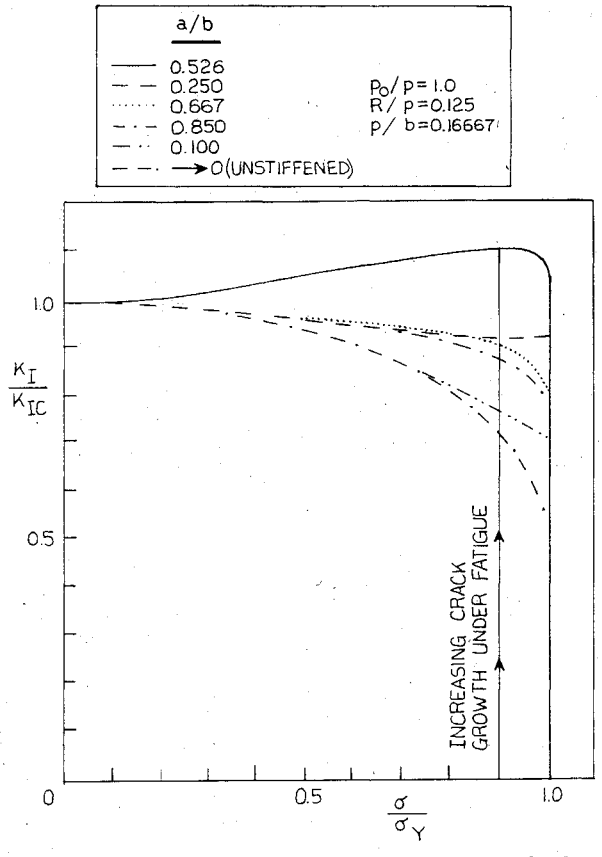

Fig. 9 Cyclic crack growth path for a stiffened panel loaded at $\sigma_{max}/\sigma_Y = 0.9$.

However, for a small crack, the experimental fracture stress would be higher and the ratio of σ/σ_Y becomes closer to one. The fracture would be more likely to occur under net section yielding with the ductility effect increasing, and LEFM does not give as accurate a result as does the fracture diagram.

Fatigue Life of a Stiffened Panel as Evaluated with a Fracture Diagram

The fatigue life of a stiffened panel is an important piece of knowledge to those who design aerospace structures. In an attempt to gain some insight into the effect of ductility upon the fatigue life of a stiffened panel, the following theoretical work was performed. It is the first such fatigue study known to make use of the fracture diagram. The fatigue life of a stiffened panel was determined for two different catastrophic fracture criteria: the fracture diagram and LEFM. Two different crack growth laws were used to determine crack propagation in a stiffened panel under constant amplitude cyclic loading, 0 to σ_{max}.

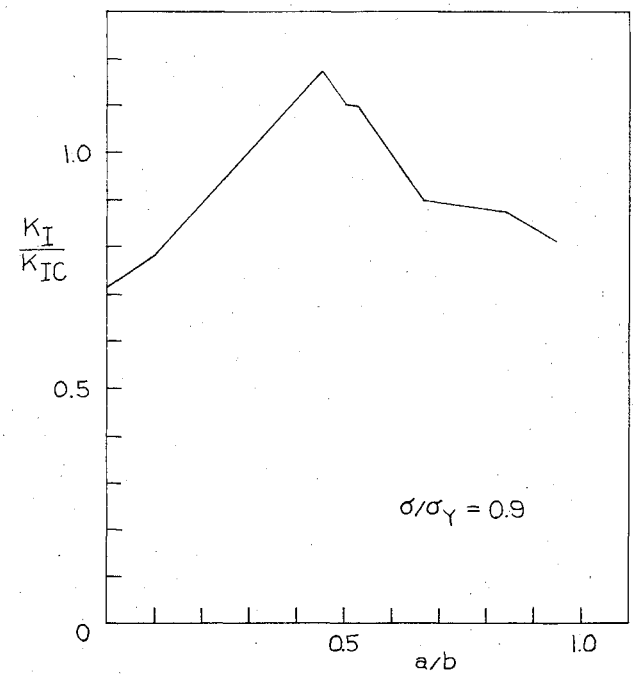

Fig. 10 Critical K_I/K_{IC} vs a/b for the twin stiffened panel via the fracture diagram.

Paris' law[12]

$$\frac{da}{dN} = C_p(\Delta K)^n \tag{10}$$

Forman's law[13]

$$\frac{da}{dN} = \frac{C_F(\Delta K)^m}{(1-\mathcal{R})K_{IC} - \Delta K} \tag{11}$$

The constant coefficients, C_p and n from Paris' equation and C_F and m from Forman's equation, depend upon the material composition and service conditions. $\mathcal{R}$ is the ratio of K_{min} to K_{max}. Numerical integration was used to determine the number of cycles N to failure from a given small flaw for different crack growth laws. A computer subroutine was developed to determine this remaining useful life of a stiffened panel. The computer code determined the critical crack size as well as the number of cycles for each increment of crack size. In the end, it evaluated the total number of cycles for the crack to propagate from subcritical size to the critical ıze. The crack size was incremented by taking the difference between the width of the specimen and the initial crack size and then dividing by the desired number of intervals. The fracture criteria was evaluated by checking the value K_I/K_{IC} from analytical solutions for each crack increment against K_I/K_{IC} from the fracture diagram.

The criterion of the fracture diagram was employed by drawing a vertical line from $\sigma/\sigma_Y = 0.9$ across different values of a/b in the fracture diagram curves, as shown in Fig. 9. The resulting values of critical K_I/K_{IC} vs a/b for the specific σ/σ_Y at fracture is shown in Fig. 10. Because of the irregularity of the curve, a polynomial curve fit did not give a good approximation. The best approximation was judged to be a linear interpolation of discrete data points on the curve. This

Table 2 Critical crack sizes, in.

	a_1	a_2	a_3
LEFM	1.96	5.26	9.12
Fracture diagram	1.17	4.5	7.5

Table 3 Theoretical fatigue life for a stiffened panel, cycles to failure

	Paris' law	Forman's law
LEFM	34,150	36,867
Fracture diagram	25,795	22,949

tabulated data was stored in the computer as critical K_I/K_{IC} vs a/b. This value was checked against the value of K_I/K_{IC} as defined from the elasticity solution for each crack increment.

The fracture criteria in terms of LEFM was determined by standard means from Eq. (8).

$$K_I = K_{IC} \tag{12}$$

The critical crack size a_c was evaluated from the roots of the function

$$K_I - K_{IC} = 0 \tag{13}$$

As an example, two material properties, σ_Y and K_{IC}, were arbitrarily chosen as $\sigma_Y = 517$ MNm^{-2} (75 ksi), $K_{IC} = 181$ MN m$^{-3/2}$ (165 ksi $\sqrt{\text{in.}}$). The constant coefficients of the Paris and Forman equations were selected as follows: $C_p = 1.56 \times 10^{-7}$, $n = 2.00$, $C_F = 1.7 \times 10^{-5}$, and $m = 2.461$ consistent with the English for units a and K. A twin stiffened panel was modeled with $b = 254$ mm (10 in.) and with $\mathcal{R} = 0$.

The load ratio σ/σ_Y was selected to be 0.9 at peak amplitude, $\sigma = \sigma_{max}$. The stress intensity factors for a center cracked twin stiffened panel for fixed geometry parameters was taken from Rich and Cartright.[14] Three different critical sizes were determined from LEFM; $a_1 = 49.78$ mm (1.96 in.) $a_2 = 133.6$ mm (5.26 in.), and $a_3 = 231.6$ mm (9.12 in.). This is shown in Fig. 11 on the graph of stress intensity vs crack size a. Three separate critical crack sizes resulted from the effect of the stiffener on the stress intensity as the crack propagated. For the first case, when the crack reached a value of $a_1 = 1.96$, it became unstable. Since the distance of the stiffener from the crack was great, the stiffener did not arrest the crack immediately. However, the crack was arrested when $a_2 = 5.26$ by the stiffener. It became stable fatigue growth once more until it reached $a_3 = 9.12$ where it became an unstable crack once again. In terms of the fracture diagram, it first became unstable at 29.7 mm (1.17 in.), then it was stabilized by the stiffeners at 114.3 mm (4.5 in.), and again reached instability at 190.5 mm (7.5 in.). Table 2 summarizes the critical crack sizes using the two different failure criteria.

The total number of cycles for the crack to propagate from subcritical size, which was assumed to be zero, to the critical size was determined from both Paris' crack growth law and Forman's crack growth law. Table 3 shows the theoretical fatigue life for a stiffened panel using LEFM and a fracture diagram approach.

Comparison of the fatigue lives as predicted by LEFM and the fracture diagram shows that the total number of cycles using LEFM is significantly higher than that from the fracture diagram. A study of these results reveals some interesting insight into the role of ductility on the theoretical fatigue life of a stiffened panel. Observe that the two critical crack sizes at the onset of rapid crack propagation, a_1 and a_3, proved to be measurably smaller as predicted by the fracture diagram than the corresponding critical crack sizes as predicted by LEFM. This is because in one case, a_1, the critical crack size was reached well short of the stiffener, and in the second case,

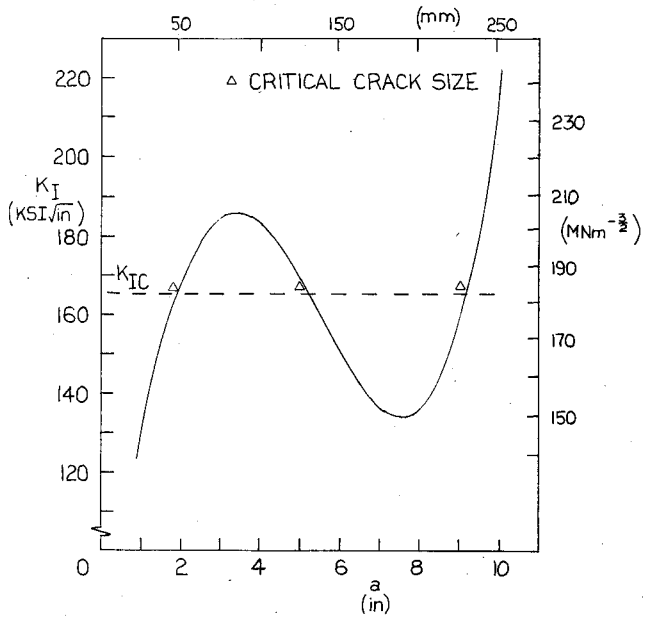

Fig. 11 Stress intensity factors and critical crack sizes from LEFM for stiffened panels ($\sigma/\sigma_Y = 0.9$ and $\mu = 0.5$).

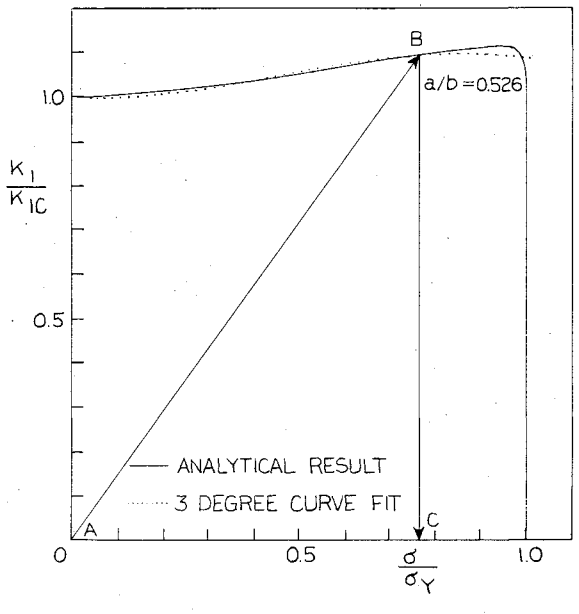

Fig. 12 Critical load determination for a stiffened panel.

a_3, it was reached well beyond. Therefore, for the load cycling at $\sigma_{max}/\sigma_Y = 0.9$, failures were predicted outside the a/b range of benefit, which is near $a/b = 0.526$. Hence, in this example, ductility effects upon rupture caused the rapid crack growth to begin at values of K_I/K_{IC} nearer to 0.8 on the fracture diagram rather than 1.0 as used in LEFM computations.

The result of this ductility effect at an admittedly high value of σ/σ_Y was to shorten the fatigue life as both a_1 and a_3 were reached sooner via the fracture diagram criterion. It is interesting to note that the crack arrest size a_2 was indeed smaller as predicted by the fracture diagram than that from LEFM. This is because the intermediate crack instability size occurred near the stiffener at around $a/b = 0.5$, and the fracture diagram limited failure at $K_I/K_{IC} > 1.0$. However, this effect of lowering the starting crack size for fatigue computations in the second fatigue growth region could not compensate for the ductility effects upon a_1 and a_3.

As a final note, given a flaw of some specified size with a stiffened panel, the critical load is determined in the same manner as earlier described for the unstiffened case. Referring to Fig. 12, the slope of the load path can be obtained from the analytical solution for K_I of the stiffened panel and Eq. (7). Point B is located at the intersection of the load path and the appropriate fracture diagram defining the critical load ratio, σ_f/σ_Y at point C. Since the yield strength of the sheet material is presumed to be known, the critical loading stress is obtained.

References

[1]Dugdale, D.S., "Yielding of Steel Sheets Containing Slits," *Journal Mechanics and Physics of Solids,* Vol. 8, 1960, pp. 100-104.

[2]Rich, T.P., Ghassem, M.M., and Cartwright, D.J., "A Generalized Fracture Diagram for 2-D, Elastic-Plastic, Mode I Failure," under revision for *Engineering Fracture Mechanics.*

[3]Westergaard, H.M., "Bearing Pressures and Cracks," *Journal of Applied Mechanics,* June 1939, pp. A49-A53.

[4]Paris, P.C. and Sih, G., "Stress Analysis of Cracks," *ASTM Special Technical Publication No. 381,* American Society for Testing and Materials, 1965, pp. 30-83.

[5]Burdekin, F.W. and Stone, D.E.W., "The Crack Opening Displacement Approach to Fracture Mechanics in Yielding Materials," *Journal of Strain Analysis,* Vol. 1, 1966, pp. 145-153.

[6]Poe, C.C., "Stress Intensity Factors for a Cracked Sheet with Riveted and Uniformly Spaced Stringers," *NASA TR R-358,* May 1971.

[7]Cartwright, D.J. and Rich, T.P., "Plastic Strip Yielding for a Crack in a Stiffened Sheet," *Numerical Methods in Fracture Mechanics,* University College of Swansea, Swansea, Wales, Jan. 1978, pp. 550-568.

[8]Ghassem, M.M., *Fracture Diagram for Stiffened Panel and Computer Based Approach for Structural Life Prediction,* Ph.D. Dissertation, Mechanical Engineering Department, Texas A&M University, College Station, Texas, Aug. 1980.

[9]Wells, A.A., "Unstable Crack Propagation in Metals: Cleavage and Fast Fracture," Cranfield Crack Propagation Symposium I, Sept. 1961, p. 210.

[10]Harrison, R. P., Loosemore, K., and Milne, I., "Assessment of the Integrity of Structures Containing Defects," *R/H/R6-Rev 1,* Central Electricity Generating Board, Research Division, London, 1977.

[11]Feddersen, C. E., "Evaluation and Prediction of the Residual Strength of Center Crack Tension Panel," *ASTM Special Technical Publication No. 486,* American Society for Testing and Materials, 1971.

[12]Paris, P. C., Gomez, M. P. and Anderson, W. E., "A Rational Theory of Fatigue," *The Trend in Engineering,* Vol. 39, 1967.

[13]Forman, R. G., Kearney, V. E., and Engle, R. M., "Numerical Analysis of Crack Propagation in a Cyclic Load Structure," *Journal of Basic Engineering,* 88D, 1967, p. 549.

[14]Rich, T. P. and Cartwright, D. J., private communications, University of Southampton, Southampton S09 5NH, England, 1979.